Available online at www.sciencedirect.com
SCIENCE DIRECT®
C. R. Mecanique 332 (2004) 387–396
COMPTES RENDUS MECANIQUE

Microgravity and Transfers/Combustion, chemical reactivity

Different spreading regimes of spray-flames

Sylvain Suard, Pierre Haldenwang, Colette Nicoli

Modélisation et simulation numérique en mécanique, FRE 2405 du CNRS, IMT/La Jetée/L3M, 38, avenue Joliot Curie, 13451 Marseille cedex 20, France

Available online 24 April 2004

Abstract

We present a minimal model of spray combustion to investigate a flame front propagating through a fuel-lean mixture of fuel vapor, droplets and air. The model relies on a main control parameter, *Da*, named the Damkoehler number, which allows us to take into account a large variety of fuel sprays. Numerical results reveal, as a function of *Da*, a wide range of spray-flame structures, including the classical gaseous premixed flame, a specific regime controlled by vaporisation, and a pulsating mode of propagation. The latter appears when the vaporisation is smaller than (or equal to) the reaction time, and it occurs even with a unit Lewis number. ***To cite this article: S. Suard et al., C. R. Mecanique 332 (2004).***

Résumé

Différents modes de propagation pour les flammes de brouillard. Un modéle minimal pour la combustion des brouillards est présenté. Il permet d'étudier la propagation d'une flamme à travers un milieu pauvre en hydrocarbure, constitué de vapeur, de gouttelettes et d'air. Il met en évidence, comme paramètre principal, le nombre de Damkoehler (*Da*), dont la variation nous permet d'étudier de nombreuses configurations de combustion des brouillards. Les résultats numériques font apparaître plusieurs régimes de flammes : le classique mode de propagation des flammes de prémélange gazeux, un régime spécifique contrôlé par l'évaporation et un mode de propagation pulsant. Ce dernier apparaît lorsque le taux d'évaporation est supérieur ou égal au taux de réaction chimique ($Da \leqslant \mathrm{O}(1)$), et ce, même quand le nombre de Lewis vaut un. ***Pour citer cet article : S. Suard et al., C. R. Mecanique 332 (2004).***

Keywords: Combustion; Spray combustion; Vaporisation; Pulsating flames

Mots-clés : Combustion ; Combustion des brouillards ; Evaporation ; Flammes pulsantes

Version française abrégée

La combustion des brouillards occupe une place majeure dans diverses applications industrielles telles que la propulsion aérospatiale et terrestre. Il est, de ce fait, primordial de comprendre les différents modes de propagation d'une flamme dans un brouillard de gouttelettes. Plusieurs travaux expérimentaux, [1–5] ont montré l'existence de certains aspects communs aux flammes de brouillard et aux flammes de prémélange. Cependant, certains

E-mail addresses: suard@L3M.univ-mrs.fr (S. Suard), haldenwang@L3M.univ-mrs.fr (P. Haldenwang), nicoli@L3M.univ-mrs.fr (C. Nicoli).

1631-0721/$ – see front matter
doi:10.1016/j.crme.2004.02.004

phénomènes comme la nature extrêmement plissée du front de flamme, conduisant à des anomalies de propagation [5,8,9] et comme des domaines de flammabilité inattendus [10] restent encore à élucider.

Bien que la combustion des brouillards relève de la combustion hétérogène, il est possible sous certaines hypothèses de considérer le brouillard comme un milieu homogène [11–15]. Le modèle minimal présenté ici s'inscrit dans cette approche et s'intéresse particulièrement à la propagation de flammes dans un brouillard pauvre prémélangé.

Aussi, un processus d' homogénéisation est appliqué à l'ensemble du brouillard ; cette hypotèse est valide si la plus petite échelle de longueur dans la flamme de brouillard est grande devant l'échelle d'homogénéisation. Cette situation est a priori réalisée quand E_{SF}, l'épaisseur caractéristique de la flamme de brouillard est grande devant la distance inter-goutte L_d.

Ceci permet également de supposer que la cinétique chimique ne dépend que des grandeurs macroscopiques.

Par ailleurs, d'autres simplifications classiques en combustion nous permettent de réduire notre modèle : (a) la combustion étant du type déflagration, l' hypothèse d'un écoulement à bas nombre de Mach est validée ; (b) le brouillard étant globalement pauvre, la réaction est contrôlée par une espèce limitante (le fuel). Une pression relativement basse et une hypothèse de brouillard pauvre nous permettent de considérer la distance inter-goutte grande devant R_d, le rayon des gouttes. Ainsi les interactions entre gouttes étant négligeables, nous dérivons le schéma d'évaporation de la loi de Spalding–Godsave, dite loi du « d^2 ». Plus de détails sur ces hypothèses se trouvent dans [12]. Le nombre de transfert B, appelé nombre de Spalding, est calculé à l'aide de la température de l'interface liquide-gaz, de la pression et de la fraction massique de vapeur saturante. Cependant, pour les brouillards de gouttelettes pauvres en hydrocarbure, plusieurs simplifications complémentaires peuvent être introduites : (a) aux basses températures, l'interface admet une température proche de celle du mélange gazeux ; (b) pour une température de mélange supérieure à la température d'ébullition, le terme de Spalding se comporte comme une fonction linéaire de cette température, et ce, indépendamment de la fraction massique de fuel gazeux. Ces deux points nous permettent une expression explicite du terme de Spalding.

Alors, le modèle se réduit à trois équations de conservation : deux équations pour les fractions massiques de fuel liquide (6) et gazeux (7) et une équation pour la température du mélange (8). L'adimensionnement retient, comme grandeurs de référence, l'épaisseur et la vitesse de flamme des prémélanges gazeux. Ceci conduit aux Éqs. (12), (13) et (14).

L' exploitation numérique que nous présentons se situe dans le cadre de l'approximation thermo-diffusive pour laquelle nous négligerons, de plus, les effets de diffusions différentielles (nombre de Lewis, Le, égal à l'unité). Pour une énergie d'activation standard (nombre de Zeldovich de l'ordre de dix), nous reportons les différents régimes de flammes en fonction du nombre de Damkoehler (19).

Quand le phénomène d'évaporation est de loin le plus rapide, $Da \ll 1$ (Fig. 1), la flamme de brouillard s'apparente à une flamme de prémélange gazeux. La vaporisation se produit dans la zone de préchauffage. La fraction massique réduite de fuel vapeur destinée à la combustion est proche de 1, comme dans un prémélange gazeux ordinaire.

Pour un nombre de Damkoehler plus important ($Da > 1$) (Fig. 2), le processus de vaporisation impose son échelle de temps. Une combustion résiduelle s'étend très au-delà du taux maximum de réaction. Dans cette zone à haute température, la vaporisation contrôle le taux de réaction, les profils des taux de réaction et de vaporisation étant alors confondus. La flamme de brouillard a, dans cette gamme de paramètres, deux zones bien distinctes qui ont fait l'objet de descriptions précises dans la littérature expérimentale.

Dans l'autre cas limite ($Da \gg 1$) (Fig. 3), la quantité de fuel gazeux disponible devient de plus en plus faible. Les profils de réaction et d'évaporation étant pratiquement confondus, la flamme de brouillard est maintenant pilotée par un mécanisme d'évaporation–diffusion.

La Fig. 4 présente les variations de la vitesse de flamme en fonction du nombre de Damkoehler et de la fraction massique initiale de fuel en phase liquide. Pour $Da < 2$, la vitesse est très voisine de la vitesse de flamme d'un prémélange gazeux. Inversement, lorsque $Da > 10$ la vitesse de flamme chute rapidement et se comporte comme $Da^{-1/2}$ pour un fuel à très faible tension de vapeur saturante (courbe $Yl_u = 1$ sur la Fig. 4). Dans ce cas, la vitesse

dimensionnée s'avère inversement proportionnelle au rayon de la goutte. En d'autres termes, l'échelle de temps de la réaction disparaît comme temps caractéristique de transit au profit du temps d'évaporation. Bien que dans cette limite l'épaisseur de réaction–diffusion soit petite devant la distance inter-goutte, le processus d'homogénéisation garde son sens car l'épaisseur de flamme est maintenant E_{VD}, l'échelle de longueur du régime d'évaporation–diffusion. Le fait que cette dernière s'avère proportionnelle à la distance inter-goutte, assure la consistance du modèle.

Considérons maintenant la gamme des nombres de Damkoehler, $10^{-2} < Da < 1$. Bien que structure et vitesse de flamme varient très peu sur cette plage (Fig. 4) la stabilité des flammes s'y avère très sensible au nombre de Zeldovich. En effet, quand ce dernier excède une certaine valeur (> 10), la flamme accélère et décélère périodiquement (Fig. 5).

Ainsi la flamme de brouillard présente un mode de propagation pulsant. En comparaison avec les flammes gazeuses, ce comportement est ici très particulier car il ne résulte pas des effets de diffusions différentielles.

1. Introduction

Spray combustion occurs in many industrial systems such as diesel and rocket engines, turbojets or industrial furnaces. However, despite these wide applications, heterogeneous combustion with fuel–air mixtures is not yet fully understood. From the first experimental studies [1–5] one can extract a general trend: presence of droplets promotes the burning rate. More precisely, the burning velocity of a flame propagating through a fuel vapor, droplets and air mixture exceeds most of the time that of the flame propagating through an equivalent fuel vapor–air mixture. For instance, Mizutani and Nakajima [2] observed for different configurations an increase of the spray-flame velocity by the addition of droplets.

However, at the same time, Hayashi and Kumagai [3] and Hayashi et al. [5] observed the importance of the fuel–air ratio in the gas phase on the spray-flame structure and burning velocity: they noticed an important effect opposing fuel-rich and fuel-lean mixtures. Although the promotion of spray-flame for fuel-rich mixture were reported, spray-flame velocity in fuel-lean mixtures decreased with increasing droplets size or liquid fuel–air ratio. Ballal and Lefebvre [6] confirmed the latter results for iso-octane sprays at normal atmospheric pressure and an equivalent ratio of 0.65 and unity. Myers and Lefebvre [7] reported the same features when they studied the burning velocity and spray flame structures for six different fuels over a wide range of equivalence ratio. In addition, the measured burning velocity is found to be inversely proportional to mean drop size (above some critical size), those observations emphasizing that flame speed is controlled by evaporation rate. For smaller drop sizes flame speed is found independent of evaporation rate.

Further particular features of spray combustion observed through experimental studies are not elucidated. Corrugated flame fronts with cellular structures [5] appear in mixtures containing large droplets although smooth and continuous flame fronts are peculiar to mixtures with smaller size droplets. It was also demonstrated [8,9] that under certain circumstances a spray flame can be cellular when its equivalent non-spray flame is completely flat. Furthermore, the low flammability limit using low volatility liquid fuels in air [10] decreased as the droplet size increased. The flammability domain may be either smaller or larger than in the case of gaseous mixtures.

Although spray combustion is considered as heterogeneous combustion, homogeneous regimes for spray-flame can be envisaged if spray-flame thickness is larger than the length scale of non-homogeneity (i.e., the characteristic distance between droplets). This is the purpose of numerical [11,12] and theoretical [13–15] works, in which existence of travelling waves is exhibited. Polymeropoulos [11] considered a flame propagation into a quiescent combustible mixture consisting of liquid fuel droplet, fuel vapor and air. For the operating conditions, he numerically showed the existence of an optimum droplet size at which the flame speed achieves a maximum value. His further theoretical study [13], which extends [6] with a new approach of calculating burning velocities, confirmed [11]. Using asymptotic development with high activation energy, Lin et al. [14] analyzed the structure, and the propagation of a steady, low-speed flame in sufficiently off-stoichiometric dilute spray. The results showed

that lean and rich sprays exhibit opposite behavior in term of velocity enhancement effect with increasing droplets size. Through a linear stability analysis, Greenberg et al. [15] predicted an increase of the effect related to differential diffusions, which leads to pulsating cellular spray-flames.

The present paper is an extension of Suard et al. [12], a previous paper devoted to the study of homogeneous phenomena in spray combustion. Section 2 presents the different steps of the modelling proceedure while Section 3 reports numerical results on various spray-flame propagation regimes.

2. Modelling

2.1. Basic assumptions

To consider the spray as an uniform medium, a homogenization process must be applied, which consists in averaging all fields on a scale intermediate between spray-flame length scale and droplet inter-distance; this requires that both combustion and spray scales are well separated: in other words, $L_d \ll E_{SF}$ where L_d is characteristic droplet inter-distance and E_{SF} is the spray-flame thickness. As another consequence of the latter assumption, the time needed for getting a homogeneous droplet surrounded is much smaller than chemical reaction time. The presence of the liquid phase then affects the gas flow only through source or sink mean terms for the species produced or consumed around the droplets.

Additional assumptions, as classically made in combustion modelling, are:

- the combustion phenomenon is of deflagration type; therefore, we are faced with a low Mach number flow situation where gas pre-heating is controlled by thermal conduction (in absence of radiative effects);
- Fick's law for diffusion and Fourier's law for heat conduction are applied. Dufour and Soret effects are neglected;
- mixture thermal conductivity, diffusion coefficient, specific heat at constant pressure and latent heat of vaporisation can be approximated by constant values;
- all droplets have the same velocity as the host gas, (droplet inertia is neglected);
- chemical kinetics are described by a single global chemical reaction. Furthermore, the gaseous mixture surrounding the droplets here being supposed fuel-lean, reaction is controlled by a unique limiting (fuel) species (oxidant always being in excess).

2.2. Simplified evaporation scheme for fuel-lean sprays

We next consider a flame front propagating through a globally fuel-lean mixture composed of air, fuel vapor and fuel droplets. Because combustion occurs in the gas phase, the flame front is supposed to be preceded by a vaporisation front where the dispersed liquid phase produces the fuel vapor available for combustion. Let us first characterize the vaporisation process, which corresponds to the main departure of the spray-flame to the classical gaseous premixed flame. We derive the vaporisation scheme from the classical Spalding–Godsave 'D^2 law', which requires moderate pressure, nondifferential diffusion effects (unity Lewis number) and droplet inter-distance much larger than the droplet radius, R_d. These assumptions are fulfilled for conventional sprays [12]. The approach by Spalding–Godsave provides us with the following fuel vaporisation rate:

$$\dot{m}_{\text{vap}} = 4\pi r_d \frac{\lambda}{C_p} \ln(1 + B) \tag{1}$$

where r_d, λ, C_p are constant quantities, respectively, the instantaneous radius of the droplet, the surrounding air thermal conductivity, and the heat capacity. B is the so-called Spalding number, which relates the temperature

T_s and the fuel mass fraction Y_{Fs}, defined at the droplet surface, to the volume gaseous quantities, through the following relationships:

$$B = \frac{C_p}{L}(T - T_s) = \frac{Y_{Fs} - Y_F}{1 - Y_{Fs}} \tag{2}$$

The quantity T is the surrounding mixture temperature, Y_F is the gaseous fuel mass fraction, and L is the latent heat of vaporisation. Eq. (2), for a given state of the gaseous phase (i.e., for T and Y_F fixed), requires an additional relationship between T_s and Y_{Fs}: at low pressure, the latter is furnished by the Clausius–Clapeyron coexistence curve

$$\ln(X_{Fs}) = \frac{L}{R}\left(\frac{1}{T_{\text{boil}}} - \frac{1}{T_s}\right) = -\beta_{\text{vap}}\left(\frac{1-\varphi_s}{1-\gamma'(1-\varphi_s)}\right) \tag{3}$$

where X_{Fs} is the fuel molar fraction in the gaseous mixture, T_{boil} is the boiling temperature and R is the universal gas constant.

The quantity $\beta_{\text{vap}} = \gamma' L/(RT_{\text{boil}})$ is the reduced vaporisation energy, $\varphi_s = (T_s - T_u)/(T_{\text{boil}} - T_u)$ is the reduced surface temperature and $\gamma' = (T_{\text{boil}} - T_u)/T_{\text{boil}}$ is an expansion parameter. T_u is the temperature of the fresh mixture.

The gaseous fuel mass fraction is related to fuel molar fraction through

$$Y_{Fs} = \frac{X_{Fs}}{X_{Fs} + W(1 - X_{Fs})} \tag{4}$$

where W is the ratio of air molar weight to fuel molar weight.

For a given state of gaseous environment, Eqs. (2), (3) and (4) correspond to a non-linear system (to be solved iteratively) which controls the vaporisation process. For globally fuel-lean standard sprays we suggest a further simplification, which spares us this iterative resolution (to be carried out on each grid point).

For usual hydrocarbon sprays in standard conditions, β_{vap} is a nondimensional quantity in the range $4 < \beta_{\text{vap}} < 7$. Consequently, significant fuel molar fraction (Y_{Fs}) is obtained only in the range $1 - \beta_{\text{vap}}^{-1} < \varphi_s < 1$. Outside this range, vaporisation rate is weak, droplets remain in thermal equilibrium with gas ($T_s = T$) and Spalding–Godsave number B vanishes.

On the other hand, when T becomes of the order of the flame temperature, B is given by $C_p T_b/L$ (because $T_{\text{boil}} \ll T_b$). Therefore B is a large quantity which supposes that $Y_{Fs} \approx 1$ and $T_s \approx T_{\text{boil}}$. The proposed simplified model continuously relates both limit cases and is presented in detail through Eqs. (17) and (18).

Finally, it is straightforward to show that the vaporised mass rate per volume unit can be expressed:

$$\dot{\rho}_{\text{vap}} = n_d \dot{m}_{\text{vap}} = 3\frac{\rho Y_{Fl}}{r_d^2}\frac{\lambda}{\rho_l C_p}\ln(1+B) = 3[Y_{Fl}\rho]^{1/3}[Y_{Fl_u}\rho_u]^{2/3}\frac{\lambda}{\rho_l C_p R_d^2}\ln(1+B) \tag{5}$$

where n_d is the number of droplets per volume unit. Y_{Fl}, ρ and ρ_l are respectively the mass fraction of liquid fuel, the instantaneous spray density, and the liquid fuel density. Subscripts u and b refer to quantities relative to fresh and burnt mixtures, respectively.

2.3. Governing equations

Under the set of the previously mentioned hypotheses, we formulate the liquid fuel, gaseous fuel and energy conservation equations as follows

$$\frac{\partial Y_{Fl}}{\partial t} + \mathbf{U}\cdot\nabla(Y_{Fl}) = -\frac{\dot{\rho}_{\text{vap}}}{\rho} = -\dot{\varpi}(\rho, T, Y_{Fl}) \tag{6}$$

$$\frac{\partial Y_F}{\partial t} + \mathbf{U}\cdot\nabla(Y_F) = \frac{1}{\rho}\nabla\cdot\big(\rho D\nabla(Y_F)\big) - \dot{w}(\rho, T, Y_F) + \dot{\varpi}(\rho, T, Y_{Fl}) \tag{7}$$

$$\frac{\partial T}{\partial t} + \mathbf{U}\cdot\nabla(T) = \frac{1}{\rho}\nabla\cdot\left(\frac{\lambda}{C_p}\nabla(T)\right) + \frac{Q}{C_p}\dot{w}(\rho, T, Y_F) - \frac{L}{C_p}\dot{\varpi}(\rho, T, Y_{Fl}) \tag{8}$$

where D is the fuel mass diffusivity in air, Q is the heat of reaction per fuel mass unit, $\mathbf{U}$ is the local hydrodynamic velocity and $\dot{w}(\rho, T, Y_F)$ is the rate of chemical reaction, given by the Arrhenius law

$$\dot{w}(\rho, T, Y_F) = Y_F \rho_{O_2} F(T) \exp\left(-\frac{E_A}{RT}\right) \tag{9}$$

where $F(T)$ is a pre-exponential factor, taken to be constant, ρ_{O_2} the oxygen mass per volume unit, and E_A the activation energy. For general study, this set of governing equations needs to be complemented with the Navier–Stokes equations.

In order to have a nondimensional form, typical length and time scales must be introduced. The Zeldovich and Frank–Kamenetsckii analysis defines the premixed flame velocity in the limit of infinite activation energy as

$$U_L = \sqrt{\frac{2Le\lambda\rho_b^2 Y_{O_2} F(T_b)}{C_p \rho_u^2 \beta^2}} \exp\left(-\frac{E_A}{2RT_b}\right) \tag{10}$$

where Le, the Lewis number, is the ratio of thermal diffusivity to mass diffusivity and β is the reduced activation energy (so-called Zeldovich number), $\beta = (E_A/RT_b^2)(T_b - T_u)$ with T_u and T_b the temperature of the fresh and burnt mixture.

U_L, coupled with thermal diffusivity of fresh air D_u, allows us to define the length and time scales of reaction–diffusion, respectively, $E_{RD} = D_u U_L^{-1}$ and $\tau_{RD} = D_u U_L^{-2}$. Furthermore, let us define the adiabatic spray flame temperature as

$$T_b = T_u + \frac{Q}{C_p} Y_{F_u} + \frac{Q - L}{C_p} Y_{Fl_u} \tag{11}$$

This leads to define the reduced temperature as $\theta = (T - T_u)/(T_b - T_u)$. Unit of mass ρ' is related to the density of fresh mixtures ρ_u and the mass fraction is normalized with the overall fuel mass fraction of fresh mixture $\psi = (Y_F + Y_{Fl})_u$.

Eqs. (6)–(8) then give the following reduced system

$$\frac{\partial Y_l}{\partial \tau} + \mathbf{V}\cdot\nabla Y_l = -\dot{\eta} = -\left[\frac{Y_l Y_{l_u}^2}{\rho'^2}\right]^{1/3} \rho' D' \frac{\ln(1+B)}{Da} \tag{12}$$

$$\frac{\partial Y_g}{\partial \tau} + \mathbf{V}\cdot\nabla Y_g = \frac{1}{Le\rho'}\nabla\cdot(\rho' D'\nabla Y_g) - \dot{\omega} + \dot{\eta} \tag{13}$$

$$\frac{\partial \theta}{\partial \tau} + \mathbf{V}\cdot\nabla\theta = \frac{1}{\rho'}\nabla\cdot(\rho' D'\nabla\theta) + \frac{\dot{\omega} - \Lambda\dot{\eta}}{1 - \Lambda Y_{l_u}} \tag{14}$$

where D' and ρ' are the thermal diffusivity and mixture density reduced with that of fresh air, respectively. Λ is the fuel vaporisation heat reduced with the reaction heat, and Da, the Damkoehler number, is here the ratio of the typical vaporisation time to the reaction time. The reduced reaction rate admits the following classical form

$$\dot{\omega} = \frac{\beta^2}{2Le} Y_g \exp\left(\frac{\beta(\theta - 1)}{1 + \alpha(\theta - 1)}\right) \tag{15}$$

where $\alpha = (T_b - T_u)/T_b$ is a thermal expansion parameter.

With these nondimensional quantities, the Spalding number (Eq. (2)) can be written:

$$B = \beta'(\theta - \theta_s) = \frac{Y_{Fs} - \psi Y_g}{1 - Y_{Fs}} \tag{16}$$

with the reduced surface temperature: $\theta_s = (T_s - T_u)/(T_b - T_u)$ and $\beta' = C_p(T_b - T_u)/L$. As mentioned in Section 2.2 we introduce a threshold in gas temperature, below which vaporisation rate is negligible. Comparison

with the exact vaporisation scheme shows that the actual choice of the threshold value is not very sensitive (here we choose $\theta_{\text{boil}}/2$). Furthermore, our numerical experiments indicate that the results presented in Section 3 do not depend on the detailed form of the vaporisation model. This observation is shared with different contributors in spray combustion modelling [16]. We give now details on the selected simplified vaporisation model. It considers the three following temperature domains:

- If $\theta \in [0, \theta_{\text{boil}}/2]$, $B_1(\theta) = 0$
- If $\theta \in [\theta_{\text{boil}}/2, \theta_{\text{boil}}]$, $B_2(\theta) = a\theta^2 + b\theta + c$
- If $\theta \in [\theta_{\text{boil}}, 1]$, $B_3(\theta) = d\theta + e$

where a, b, c, d and e are constant parameters determined by the following continuity conditions:

$$B_1(\theta_{\text{boil}}/2) = B_2(\theta_{\text{boil}}/2), \quad B_2(\theta_{\text{boil}}) = B_3(\theta_{\text{boil}}) \quad \text{and} \quad B_3(\theta = 1) = B_{\max} = \beta'(1 - \theta_{\text{boil}}) \tag{17}$$

$$\left.\frac{\mathrm{d}B_2(\theta)}{\mathrm{d}\theta}\right|_{\theta=\theta_{\text{boil}}/2} = 0 \quad \text{and} \quad \left.\frac{\mathrm{d}B_2(\theta)}{\mathrm{d}\theta}\right|_{\theta=\theta_{\text{boil}}} = \left.\frac{\mathrm{d}B_3(\theta)}{\mathrm{d}\theta}\right|_{\theta=\theta_{\text{boil}}} \tag{18}$$

where B_{max} is the maximum value of the Spalding number (i.e., for $\theta = 1$ and $\theta_s = \theta_{\text{boil}}$).

Finally, we get the precise form of the Damkoehler number as

$$Da = \frac{\tau_{\text{vap}}}{\tau_{\text{ch}}} = \frac{1}{3}\frac{\rho_l}{\rho_u}\frac{U_L^2 R_d^2}{D_u^2} \tag{19}$$

We observe that this quantity can vary in a wide range, due to the fact that very different droplet radii and premixed flame velocities can occur in practical applications. Therefore *Da* appears as the main parameter of the present study.

3. Results and discussion

The constant density assumption, which decouples heat and species conservation laws from the Navier–Stokes equations, is a classical framework for certain fundamental studies in combustion. It is therefore interesting to point out the discrepancies between plane spray-flames and plane gaseous flames under this assumption. To avoid additional effects due to differential diffusion, we select Lewis number to be unity. In conclusion, let us study the one-dimensional spray-flame structure for $\rho' = D' = 1$.

3.1. Spray-flame structure versus Da

The aim of this section is to analyze the part played by *Da* on the spray-flame speed and related flame structure.

When the evaporation rate is the most rapid phenomenon ($Da \ll 1$), spray-flame structure (Fig. 1) can be compared to the premixed gaseous flame: vaporisation occurs in the pre-heating zone and the mass fraction of the fuel available for combustion is near unity, as in classical premixed gaseous flame. As the Damkoehler number approaches unity, the spray flame structure does not drastically change, except for a gaseous fuel mass fraction which is no longer equal to one. In addition, the locus where vaporisation occurs widens.

For a larger Damkoehler number ($Da > 1$) (Fig. 2), vaporisation process slows down and then the gaseous fuel mass fraction available for combustion becomes leaner: the reaction rate profile adopts an usual pattern composed of a peak, now become milder, followed with a tail which meets the vaporisation rate. In this intermediate case, the spray-flame exhibited two well-defined zones:

- a premixed zone where droplets evaporate (partially before burning) to produce a premixed gaseous flame with a weaker amount of fuel available;

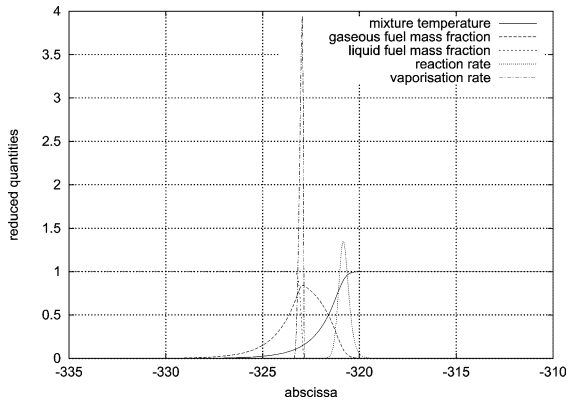

Fig. 1. $Da = 0.01$, $\beta = 8$. Spray-flame structure when the vaporisation process is more rapid than the reaction: evaporation occurs early in the pre-heating zone. The gaseous fuel mass fraction remains close to 1.

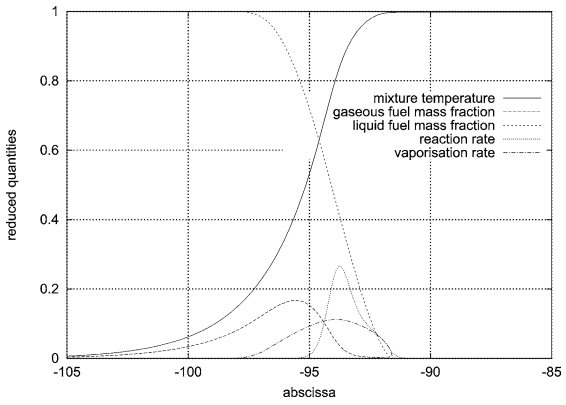

Fig. 2. $Da = 10$, $\beta = 8$. Spray-flame structure when the vaporisation is less rapid than the reaction: a first zone with non-zero gaseous fuel mass fraction (the premixed zone) and a second zone where all fuel vaporised burns immediately.

– behind this zone, droplets still evaporate with their simultaneous burning: vaporisation controls chemical reaction.

This intermediate regime has been largely described from experiments: when droplets are sufficiently large they continue to burn individually behind the flame (i.e., the peak corresponding to the premixed gaseous flame).

When $Da \gg 1$, (Fig. 3) the amount of gaseous fuel available for premixed combustion becomes weaker and weaker. As a consequence, reaction and vaporisation rates vanish (their respective profiles presented in Fig. 3 are five times magnified). In this limit case, the spray-flame is mainly driven by an evaporation–diffusion mechanism.

Let us consider now the reduced spray-flame velocity versus Damkoehler number (Fig. 4). As long as *Da* is less than (or equal to) O(1), the spray-flame exhibits the same speed as the premixed gaseous flame. From $Da = 2$ and greater, the spray-flame speed decreases as *Da* increases. These results are in agreement with experimental [5] and theoretical [14] works. The slope of this log–log profile depends on the initial amount of gaseous fuel. The minimum slope is obtained when all fuel is initially liquid; in the latter case the reduced velocity behaves like $Da^{-1/2}$. Coming back to dimensional quantities, the flame velocity is, in this limit case, proportional to D_u/R_d. In other words, the flame transit time is now proportional to the vaporisation time scale: we are faced with a vaporisation–diffusion process.

3.2. A pulsating mode for spray-flame propagation

Up to now, we have considered Zeldovich numbera less than ten. Our purpose is now to check the stability of the different observed regimes with respect to an increase of Zeldovich number.

For $\beta = 11$, as indicated in Fig. 5, the solutions obtained with $Da < 2$ exhibit an oscillatory character. This behavior is kept up to $Da < 10^{-3}$. For higher β, the existence domain (versus *Da*) of pulsating spray-flame is found slightly broader. Furthermore, the domain of pulsating spray-flame remains unchanged for vanishing latent heat.

As discussed in the preceding paragraph, in the range $10^{-3} < Da < 2$, spray-flame is comparable to gaseous premixed flame. However, in view of the existence of a pulsating mode, the comparison appears limited because gaseous premixed flames are known to be always stable for a unit Lewis number [17].

Moreover, the existence domain of pulsating spray-flame we have found is not in agreement with the analytical study reported in [15]. The authors developed a linear stability analysis specific to a homogeneous spray-flame in a similar way as [17] and plane spray-flames are found stable for unity Lewis number. For the time being, we are not

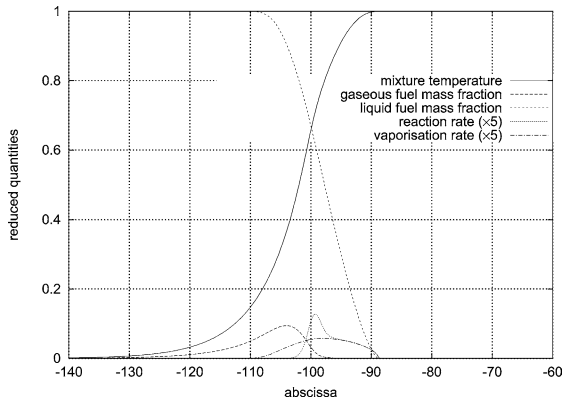

Fig. 3. $Da = 100$, $\beta = 8$. Spray-flame structure for a very slow vaporisation process: the spray-flame is driven by an evaporation–diffusion mechanism. Reaction and vaporisation rates are five times magnified.

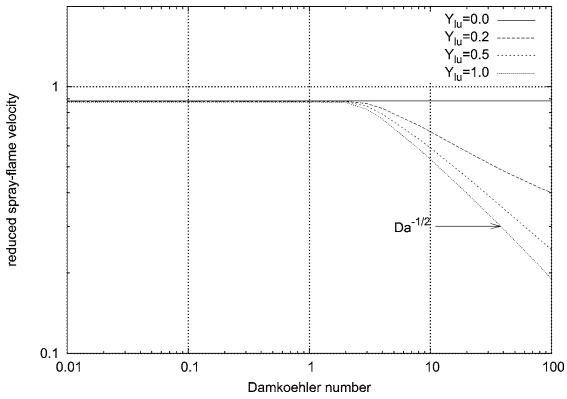

Fig. 4. Spray flame speed versus Damkoehler number for different initial liquid fuel mass fractions: for a rapid vaporisation spray-flame behaves as premixed flame, while at low vaporisation flame speed is in inverse ratio to droplet radius.

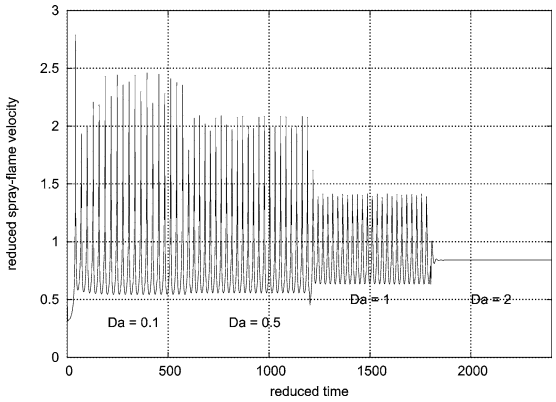

Fig. 5. $Ze = 11$, $Le = 1$ and $Y_{lu} = 1$. Time variation of reduced spray flame velocity for Da = 0.1, 0.5, 1 and 2.

able to point out the origin of this discrepancy (maybe the spray-flame structure for non-zero Damkoehler number calculated in [15] could be invoked).

On the other hand, Berthonnaud et al. [18], have analyzed the stability of plane spray-flame in the limit of vanishing Damkoehler number and unity Lewis number: they proved linear and non-linear stability for this limit case. It turns out that the latter result is not in contradiction with the present study because we also found this limit stable.

It remains to explain why a pulsating flame is observed in our simulation. It is well known that a deficient mass diffusivity leads to a pulsating flame (more precisely if the Lewis number is larger than a critical value, itself larger than 1). The fact that part of the fuel is under liquid phase makes this amount escape from mass diffusional process (according to our model). This phenomenon tends to increase the overall Lewis number of the limiting species and might be the origin of pulsating spray-flame.

4. Conclusion

We have presented an investigation of flame front-propagation through a fuel-lean mixture of fuel vapor, droplets and air. We believe that the minimal model we have used here contains the basic ingredients for a relevant study in spray-flame propagation. As a result, several modes of spray-flame propagation have been exhibited:

(a) a homogeneous propagation mode for a fuel-lean mixture with droplets of very small size (i.e., the limit case $Da \to 0$); the classical picture of a premixed gaseous flame is recovered, provided that a vaporisation front precedes the reaction zone early in the pre-heating zone;
(b) for slightly larger Da, and $Da < 2$, the previous spray-flame structure becomes unstable leading to a pulsating propagation mode (obtained even for $Le = 1$);
(c) for $Da \gg 1$ (i.e., in presence of large droplets), a vaporisation controlled regime of spray combustion occurs. The chemical reaction is constrained to run at the same pace as the vaporisation which is now the slowest process.

Propagation regime (b) appears specific to spray-flames and deserves further investigations, especially in the framework of cellular fronts because this pulsating mode is an interesting candidate for explaining several unexpected phenomena in fuel-lean spray flames.

References

[1] J.H. Burgoyne, L. Cohen, The effect of drop size on flame propagation in liquid aerosols, Proc. Roy. Soc. London Ser. A 225 (1954) 357–392.
[2] Y. Mizutani, A. Nakajima, Combustion of fuel vapor-drop–air systems. 1. Open burner flames combus, Flame 20 (1973) 343–350.
[3] S. Hayashi, S. Kumagai, Flame propagation in fuel droplet-vapor–air mixtures, in: Fifteenth Symposium (International) on Combustion, The Combustion Institute 15 (1974) 445–452.
[4] C.E. Polymeropoulos, S. Das, Effect of droplet size on burning velocity of kerosine–air sprays, Combust. Flame 25 (1975) 247–257.
[5] S. Hayashi, S. Kumagai, T. Sakai, Propagation velocity and structure of flames in droplet-vapor–air mixtures, Combust. Sci. Tech. 15 (1976) 169–177.
[6] D.R. Ballal, A.H. Lefebvre, Flame propagation in heterogeneous mixtures of fuel droplets, fuel vapor and air, in: Eighteenth Symposium (International) on Combustion, The Combustion Institute 18 (1981) 321–328.
[7] G.D. Myers, A.H. Lefebvre, Flame propagation in heterogeneous mixtures of fuel drops and air, Combust. Flame 66 (1986) 193–210.
[8] J.B. Greenberg, A.C. McIntosh, J. Brindley, Instability of a flame front propagating through a fuel-rich droplet-vapour–air cloud, Combust. Theory Modelling 3 (1999) 567–584.
[9] F. Atzler, Fundamental studies of aerosol combustion, Ph.D. thesis, School of Mechanical Engineering, University of Leeds, 1999.
[10] S. Hayashi, T. Ohtani, K. Iinuma, S. Kumagai, Limiting factor of flame propagation in low-volatility fuel clouds, in: Eighteenth Symposium (International) on Combustion, The Combustion Institute 18 (1981) 361–367.
[11] C.E. Polymeropoulos, Flame propagation in a one-dimensional liquid fuel spray, Combust. Sci. Tech. 9 (1974) 197–207.
[12] S. Suard, C. Nicoli, P. Haldenwang, Vaporisation controlled regime of flames propagating in fuel-lean sprays, J. Phys. IV 11 (2001) 301–310.
[13] C.E. Polymeropoulos, Flame propagation in aerosols of fuel droplets, fuel vapor and air, Combust. Sci. Tech. 40 (1984) 217–232.
[14] T.H. Lin, C.K. Law, S.H. Chung, Theory of laminar flame propagation in off-stoichiometric dilute sprays, Int. J. Heat Mass Transfer 31 (1988) 1023.
[15] J.B. Greenberg, A.C. McIntosh, J. Brindley, Linear stability of laminar premixed spray flames, Proc. Roy. Soc. London Ser. A 457 (2001) 1–31.
[16] G.M. Faeth, Evaporation and combustion of sprays, Prog. Energy Combust. Sci. 9 (1983) 1–76.
[17] G. Joulin, P. Clavin, Linear stability analysis of nonadiabatic flames: diffusional-thermal model, Combust. Flame 25 (1979) 247–257.
[18] P. Berthonnaud, K. Domelevo, J.-M. Roquejoffre, Stability of travelling wave solutions in a one dimensional two-phase flow combustion model, in preparation.